Observation of Flow Regime from Bubbly to Jet Flow in the Air Injection Experiment

Jongwoong Yoon, Yong Hoon Jeong*
Department of Nuclear and Quantum Engineering, Korea Advanced Institute of Science and Technology, 291 Daehak-ro, Yuseong-gu, Daejeon 34141, Republic of Korea
**Corresponding author: jeongyh@kaist.ac.kr*

1. Introduction

The ultimate goal in the nuclear safety is to prevent the release of the radioactive materials into the environment. In the severe accident conditions, the fission products are transported in the form of an aerosol. Pool scrubbing is a method that is injecting the aerosol gas into the water to filter the aerosol particles.

Much research has been performed about the pool scrubbing in the nuclear field. However, most of the previous studies were focused on decontamination factor (DF) calculation and measurement. Furthermore, the computer code such as SPARC90 and BUSCA had limitation for the high-velocity injection flow [1~2].

In this study, an experimental observation was conducted for the air injection flow by a single vertical nozzle in a water pool. Bubble behavior was visualized by using the high-speed camera, and local parameters such as void fraction and bubble velocity were measured by using the double-sensor optical fiber probe (OFP) [3].

2. Experimental method

The same test facility from the previous study was utilized [4]. It consists of two parts, a water pool and air injection system. Two different water pools, one with the 250 mm width and the other with 25 mm width were the test section. 25 mm is the equivalent diameter of the secondary side tube bundle sub-channel in the steam generator of typical PWR. The small pool with 25 mm width is called the square channel in this paper. The water pool was made of transparent acryl for the visualization.

The air was injected through the single vertical nozzle at the bottom of the pool in the center. The diameter of the nozzles were 1 mm. The mass flow controller (MFC) was used to adjust the air injection flow rate. The range of the air was 0.1 ~ 200 liter/min. Table 1 presents the air injection flow rate when the nozzle diameter was 1 mm. Weber number (We) was used as a parameter that represents the air flow rate in the experiment.

A high-speed camera was used to visualize the bubble behavior in the injection zone at the bottom of the pool. The resolution of the image was 1280 x 1024 pixels and the frame rate was 2000 frame per second. An LED backlight was used as a light source.

The double-tip OFP was used to measure the local bubble parameters. OFP detects the change of the refractive index of the light signal between air and water so it can discriminate the interface of the two-phase flow. It consists of the front sensor and rear sensor. Only the front sensor in the upstream was used to measure the void fraction since the front sensor could disturb the bubble path during the contact and distort the signal of the rear sensor. The bubble velocity was measured by the ratio of the distance between two sensors and the time difference that bubble contact two sensors. The sampling rate of the OFP was 3226 samples/sec.

Table 1. Air Injection Condition

Weber number	Air velocity [m/sec]	Injection flow rate [liter/min]
10^2	2.70	0.13
10^3	8.54	0.40
10^4	27.02	1.27
10^5	85.44	4.03
10^6	270.17	12.73
10^7	858.66	40.46

3. Observation results

3.1. Visualization of the injection flow

Figure 1 shows the visualization of the air injection flow into the water pool as the airflow rate increases. The water level was 25cm. The cross-sectional area of the water pool was 25 x 25 cm^2, and the inlet nozzle diameter was 1 mm.

The airflow rate was given in the Weber number conditions. In the Weber number 10^2 case, a single bubble generated from the nozzle and rose upward periodically. As the airflow rate increases, injected bubble size also increases. The bubble detached from the nozzle collided and merged with the next upcoming bubble.

Weber number 10^4 case shows that the bigger bubbles formed at the nozzle compared to the lower Weber number cases. However, the bubbles break into small bubbles as they rise.

Weber number 10^5 is a typical criterion that the bubbly flow transformed into the jet flow regime. For the Weber number 10^5 case in figure 1, air plume was generated from the nozzle and surface of the bubble became wavy shape. The bubble with a wavy surface is one of the characteristics of the jet flow.

For the Weber number 10^6 case, continuous bubble jet rises from the air nozzle, and for the 10^7 case, the air jet elongated from nozzle to the water surface.

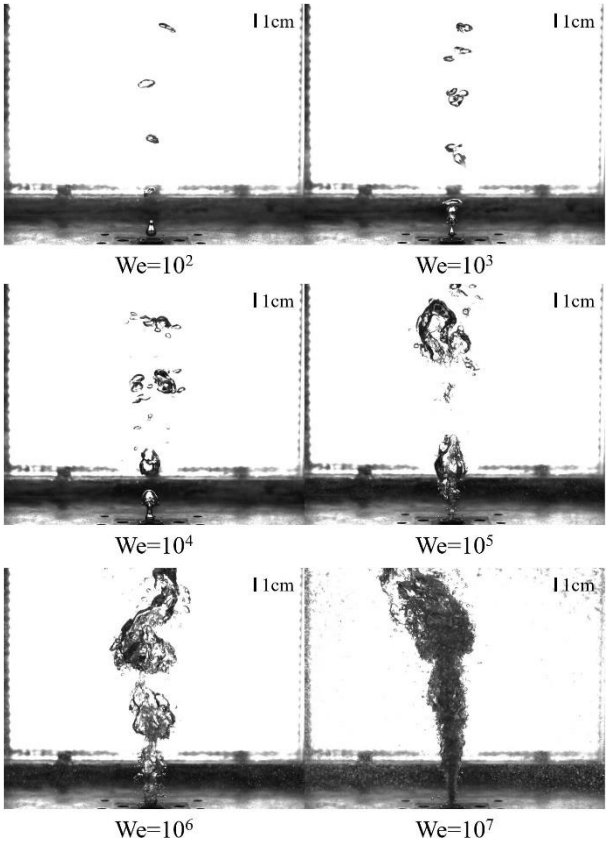

Fig. 1. Airflow visualization of the injection zone in the pool

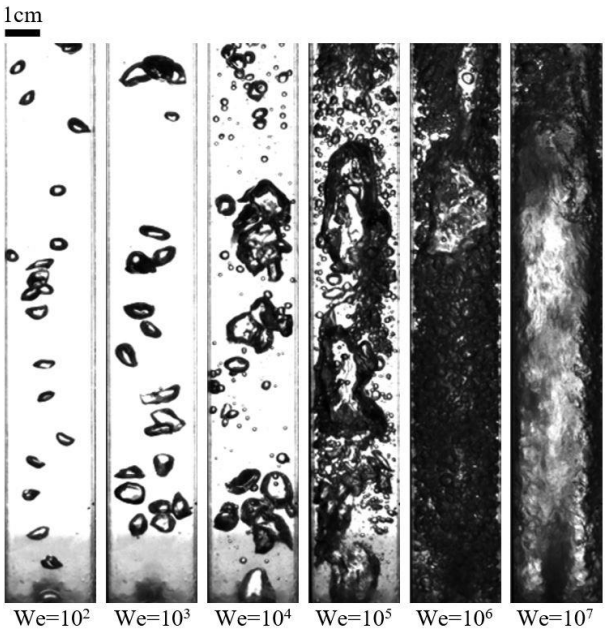

Fig. 2. Airflow visualization of the injection zone in the square channel

Figure 2 shows the visualization of the air injection into the square channel for the weber number conditions. The cross-sectional area of the square channel was 25 x 25 mm^2, and the nozzle diameter was 1 mm. The water level was 25 cm.

For the Weber number 10^2 case, a single bubble rises along the channel. As the airflow rate increases, the bubble size becomes bigger. For the Weber number 10^4 conditions, the bubbles coalesced together while they rise along the channel.

In the Weber number 10^5 case, elongated air plume generated from the nozzle. The Taylor bubble formed as the air rise through the channel. In the Weber number 10^6 case, the flow regime turns into slug flow. The big Taylor bubble moves upward in the centerline of the channel, and the water flow moves downward through the outer edge of the channel. For the Weber number 10^7 case, the flow regime changes to the annular flow. It was observed that a thin water layer covered the inner boundary of the channel.

The flow structure in the square channel was different from that of the pool. The flow regime changes from bubbly flow to the slug flow for the Weber number 10^5 case. The bubble behavior and the characteristics of the flow might be changed due to the wall effect.

3.2. Local parameter measurements

Local parameters were measured by using the double-tip OFP. The measurement was conducted at 10 cm above the nozzle, and the nozzle diameter was 1 mm. The total measurement time was 20 sec, and only the front sensor was used to calculate the void fraction.

Figure 3 shows the local void fraction for the Weber number conditions. The void fraction increases as the air flow rate increases for both the pool and the square channel case. Under the pool condition, the void fraction increases gradually in the low Weber number case and increase rapidly in the jet injection regime. For the square channel conditions, the void fraction increase dramatically in the Weber number 10^5 conditions, which is the transition point form bubbly to slug flow.

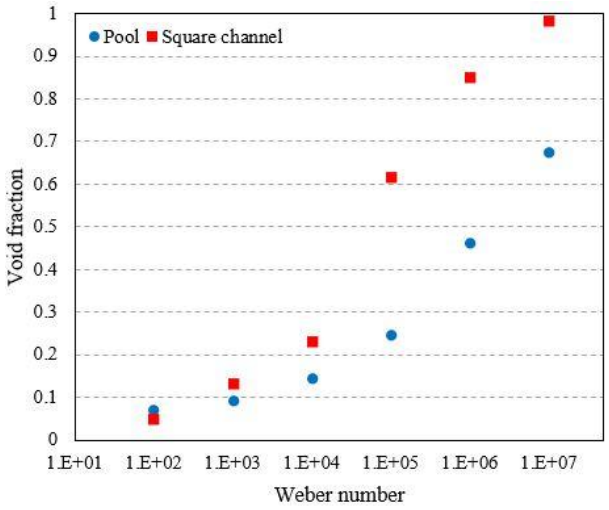

Fig. 3. The local void fraction at the injection zone

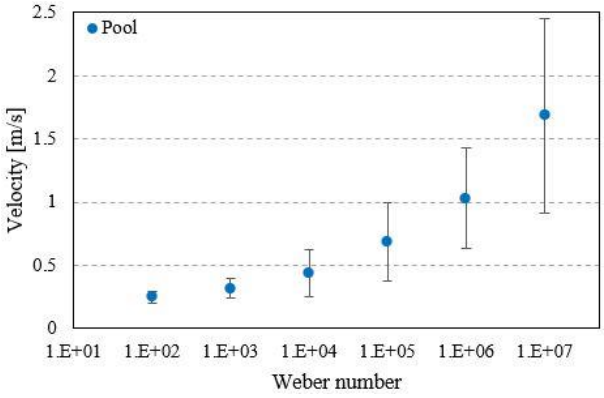

Fig. 4. Local bubble velocity of the pool

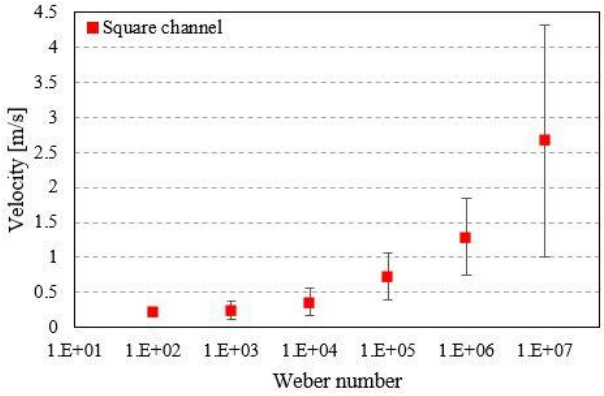

Fig. 5. Local bubble velocity of the square channel

The bubble velocity was measured simultaneously with the void fraction measurement. The distance between the front and the rear sensor was 2.007 mm, and the sampling speed was 3226 samples/sec.

Figure 4 and 5 shows the local bubble velocity under pool condition, and square channel condition respectively. The vertical error bar indicates the standard deviation for each case. As the Weber number increases, measured bubble velocity increases and its deviation also increases.

The bubble velocity of the square channel was higher than that of the pool. It is related to the flow regime and void fraction. The wall effect may influence this phenomenon.

4. Conclusions

In this study, air injection flow into the water pool using the single vertical nozzle was observed experimentally. Visualization was conducted with a high-speed camera, and double-tip OFP was used to measure the local void fraction and bubble velocity. The flow regime changed as the Weber number (i.e., airflow rate condition) increased. The wall effect was observed that bubble parameters had a different trend under the same Weber number conditions. These results could be applied to analyze the flow characteristics under pool scrubbing conditions.

ACKNOWLEDGMENTS

This work was supported by the Korea Institute of Energy Technology Evaluation and Planning (KETEP) grant funded by the Korean government (Ministry of Trade, Industry and Energy) (No. 20171510101970).

REFERENCES

[1] Dehbi, A., D. Suckow, and S. Guentay. "Aerosol retention in low-subcooling pools under realistic accident conditions." Nuclear Engineering and Design 203.2-3 (2001): 229-241.
[2] Owczarski, P. C., and K. W. Burk. SPARC-90: A code for calculating fission product capture in suppression pools. No. NUREG/CR-5765; PNL-7723. Nuclear Regulatory Commission, Washington, DC (United States). Div. of Regulatory Applications; Pacific Northwest Lab., Richland, WA (United States), 1991
[3] Le Corre, J-M., et al. "Benchmarking and improvements of measurement techniques for local-time-averaged two-phase flow parameters." Experiments in fluids 35.5 (2003): 448-458.
[4] J. Yoon et al. "Preliminary observation of air bubble behavior in the vertical square pipe under pool scrubbing conditions." Korea Nuclear Society autumn conference 2018.